Int. J. Electrochem. Sci., 11 **(2016)** 8827 – 8847, doi: 10.20964/2016.10.22

International Journal of ELECTROCHEMICAL SCIENCE
www.electrochemsci.org

Corrosion Inhibition of Low Carbon Steel by *Strychnos nux-vomica* Extract as Green Corrosion Inhibitor in Hydrochloric Acid Solution

N. Soltani[*], *N. Tavakkoli, M. Ghasemi*

Department of Chemistry, Payame Noor University, P.O. Box 19395-3697 Tehran, Iran
[*]E-mail: nasrin.soltani@pnu.ac.ir, nasrin_soltani2056@yahoo.com

Received: 1 April 2016 / *Accepted:* 4 August 2016 / *Published:* 6 September 2016

In this study, the inhibition action of *Strychnos nux-vomica* extract on the corrosion of carbon steel in 4 % and 8 % HCl solution has been investigated in different temperatures. For this purpose, the methods of weight loss, electrochemical impedance spectroscopy (EIS) and potentiodynamic polarization were used for investigation of performance of *Strychnos nux-vomica* extract in ambient temperature, while potentiodynamic polarization method was also used at different temperatures to define the effect of temperature on the inhibition efficiency of *Strychnos nux-vomica* extract. The obtained results demonstrate that inhibition efficiency in both media increased with increasing concentrations and decreases with increasing temperature. The polarization curves revealed that *Strychnos nux-vomica* extract represent mixed-type behavior in both 4 % and 8 % HCl solution. At all temperatures, the adsorption of the extract components onto the steel surface was followed Langmuir adsorption isotherm. Quantum chemical calculations were done to predict the adsorption of main components of *Strychnos nux-vomica* extract on the metal surface.

Keywords: Carbon steel; Weight loss; EIS; Polarization; Acid corrosion; *Strychnos nux-vomica* extract.

1. INTRODUCTION

Carbon steel is one of the metals, which are widely used as pipeline materials in the oil and gas industry. The use of acidic solutions for cleaning industrial, oil well acidification and petrochemical processes are very common [1]. Carbon steel, especially in acidic environments is highly sensitive to corrosion [2]. Metals used in industrial applications are protected against corrosion in many different ways. The use of corrosion inhibitors is one of the most practical methods, especially in acidic environments [3]. Organic inhibitors are compounds contains at least one functional group which

through that can be absorbed into the metal surface. Some organic compounds containing N, S and O atoms such as 3-amino-1,2,4-triazole-5-thiol [4], N-alkyl-sodium phthalamates [5], 1,4-di[1′-methylene-3′-methyl imidazolium bromide]-benzene [6], 1-(2-ethylamino)-2-methylimidazolin [7], Schiff bases [8], tris(benzimidazole-2-ylmethyl)amine [9], pyrimidothiazine derivative [10], 2-mercaptobenzimidazole [11, 12], 1H-pyrrole-2,5-dione derivatives [13] have been reported as appropriate corrosion inhibitors for carbon steel in acidic media. In recent years, due to increased environmental warnings and needs to develop environmentally friendly corrosion inhibitors, the researchers have been great attention to natural products derived from plants [14-17]. The importance of research in this field is that the natural herbal products in addition to being eco-friendly and environmentally acceptable, they are inexpensive, easily available and also renewable. Among the large number of plants, some of them, such as aqueous extract of *Hibiscus rosa-sinensis Linn* [15], leaf extracts of *Dacryodis edulis* [18], *Osmanthus fragran* leaves extract [19], the aqueous extract of olive (*Olea europaea* L.) leaves [17], aqueous extracts of mango, orange, passion fruit and cashew peels [20] and alkaloids extract from *Palicourea guianensis* plant [21] have been reported as corrosion inhibitor of carbon steel in corrosive environments. The main base of plant extracts contain compounds such as sugar, flavonoids, ellagic acid and gallic acid. The presence of mentioned compounds as well as compounds such as cellulose, tannins and polycyclic compounds can be cause higher probability for forming a film on the metal surface, so corrosion is reduced [22]. *Strychnos nux-vomica* L. (Loganiaceae), including plant that is used extensively in traditional medicine. *Strychnos nux-vomica* L. is commonly grown in South Asian countries [23]. Strychnine and brucine are main bioactive components of *Strychnos nux-vomica* L. that often used in the treatment of traumatic pain, vomiting and nervous diseases[24]. The purpose of this work is to evaluate the corrosion inhibition effect of extracts of seeds of *Strychnos nux-vomica* L. for carbon steel in 4 % and 8 % HCl solutions using weight loss, potentiodynamic polarization and AC impedance methods. Moreover, thermodynamic and kinetic parameters were obtained and discussed.

2. EXPERIMENTAL

2.1. Materials preparation

Chemical composition of low carbon steel used in this study was obtained using a SPECTROLAB quantometer and the results include: (wt. %) C (0.18), Si (0. 35), Mn (0.77), P (0.03), S (0.035) and Fe (balance). Carbon steel was in the form of strips with a thickness of 0.2 cm and a length of 5 cm. So, initially carbon steel strips were cut into pieces coupons with dimensions 1 cm × 1 cm × 0.2 cm. Pieces coupons with a small hole in the corner were used for weight loss measurements, while pieces that sealed by epoxy resin and have exposure surface 1 cm^2 were used in the electrochemical measurements. Before all experiments, carbon steel samples using emery papers with grit of 240, 400, 800 and 1200 were abraded, respectively. Then samples in ethanol were degreased and finally were washed with distilled water.

Solutions of 4 % and 8 % HCl were prepared by dilution of an analytical grade 37% HCl by using double distilled water. *Strychnos nux-vomica* extract was obtained from the Barij Essence Pharmaceutical Company (Kashan, Iran). The process of extraction was performed based on the method that explained in previous works. [23, 25, 26]. *Strychnos nux-vomica* dry seeds, ground to a very fine powder are obtained. 5.0 g of powder obtained with 20 ml of methanol was refluxed for 30 minutes while stirring. The resulting solution was filtered through Whatman no. 1 filter paper into a 25mL volumetric flask. The remaining materials on the filter paper was washed with methanol and the washing solution was added to the volumetric flask and then brought to volume with methanol. The obtained extract was concentrated under reduced pressure at a temperature of 45 ° C and freeze-dried [23]. The resulting dry extract was used to preparation of acidic solutions containing the extract. So that 1 g of extract was dissolved in the minimum amount of 1% (v/v) methanol and then in 10 mL volumetric flask was adjusted to volume with distilled water. Fially, This stock solution with concentration of 100 g L^{-1} was diluted with 4 % and 8 % HCl solutions to 4% and 8% HCl solutions containing *Strychnos nux-vomica* extract in the concentration range of 0.5 to 2 g L^{-1}obtained.

2.2. Weight loss experiment

For weight loss tests, steel pieces that were described in section 2. 1 were suspended in the test solution with nylon monofilament at different times. The test solutions were 4 % and 8 % HCl without extract and 4 % and 8% HCl solutions containing *Strychnos nux-vomica* extract in different concentration in the range of 0.5 to 2.5 g L^{-1}. After a desired time, the piece was brought out of solution, well was washed with distilled water, was dried and weighed by using a digital balance with accuracy ±0.1 mg. All tests were performed without stirring and without de aerated the solution.

2.3. Electrochemical measurements

An electrochemical cell with three-electrode configuration was used for electrochemical measurement. Carbon steel, platinum sheet and silver–silver chloride (Ag/AgCl) electrode were working, counter and reference electrodes, respectively. The results of electrochemical measurements, including potential-time, potentiodynamic polarization, and electrochemical impedance spectroscopy (EIS) measurements were achieved by using an AUTOLAB instrument, model PGSTAT 35, equipped with General Purpose Electrochemical Software (GPES) for potential-time and potentiodynamic polarization methods and Frequency Response Analysis (FRA) software for electrochemical impedance spectroscopy (EIS) method. Electrochemical experiments were conducted so that first potential-time test was done, immediately after it EIS test and eventually polarization was performed without the electrode come out of solution. The polarization curves were recorded in the range of -500 to +500 mV relative to the corrosion potential with scan rate 0.5 mV s^{-1}. The corrosion current density values were achieved by the Tafel extrapolation method by using GPES electrochemical software. EIS measurements were recorded over a frequency range of 100 kHz to 0.1 Hz with the sinusoidal wave of 5 mV at corrosion potentials, E_{corr}. The values of charge transfer resistance R_{ct}, solution resistance R_s and doublelayer capacitance C_{dl} were defined by using FRA software from Nyqust plots.

2.4. Quantum chemical calculations

All of quantum computation were carried out by using a standard Gaussian 03 software package by complete geometry optimization [27] and molecular sketches were drawn with the GaussView 3.0. The Austin Model (AM1) method were employed for strychnine and brucine, two main components of *Strychnos nux-vomica*. The frontier molecule orbital density distribution HOMO and LUMO were used for predicting the adsorption sites and thus how to attract them to the surface.

3. RESULT AND DISCUSSION

3.1. Weight loss results

3.1.1. The effect of Strychnos nux-vomica extract concentration

Weight loss tests were carried out in the absence and presence of different concentrations of Strychnos nux-vomica extract after 2 h of immersion of steel pieces in 4 % and 8 % HCl solution. Corrosion rate (ν) surface coverage (θ) and inhibition efficiency $\eta_W(\%)$ from weight loss are calculated by [28, 29]:

$$\nu = \frac{(m_1 - m_2)}{(S \times t)} \quad (1)$$

$$\theta = \frac{(\nu_0 - \nu)}{\nu_0} \quad (2)$$

$$\eta_w(\%) = \frac{(\nu_0 - \nu)}{\nu_0} \times 100 \quad (3)$$

where m_1 is the mass of steel piece before corrosion, m_2 the mass of steel piece after corrosion, *S*, the total area of steel piece, *t*, corrosion time , ν_0 and ν are the corrosion rates of steel piece in uninhibited and inhibited acid solution, respectively. The values of corrosion rates, surface coverage and inhibition efficiency were calculated using Eq. (1) to Eq. (3) and results are shown in Table 1. The experiments were repeated three times to ensure reproducibility and the averaged results are entered in Table 1.

Table 1. Corrosion parameters for carbon steel in 4 % and 8 % HCl solutions in the absence and presence of various concentrations of *Strychnos nux-vomica* extract, from weight loss method, after 2 h at 25 ºC.

Concentration (g L^{-1})	4 % HCl			8 % HCl		
	v (mg cm^{-2} h^{-1})	θ	η_W (%)	*v* (mg cm^{-2} h^{-1})	θ	η_W (%)
Blank	0.112	-	-	0.143	-	-
0.5	0.029	0.741	74.1	0.044	0.692	69.2
1.0	0.021	0.821	82.1	0.029	0.797	79.7
1.5	0.014	0.873	87.3	0.022	0.846	84.6
2.0	0.011	0.911	91.1	0.017	0.881	88.1

2.5	0.010	0.912	91.2	0.016	0.882	88.2

As the results of Table 1 demonstrate, with increasing concentrations of *Strychnos nux-vomica* extract corrosion rate were decreased and inhibition efficiency were increased. The reason for this behavior is that by increasing concentration of *Strychnos nux-vomica* extract the adsorption of molecules, existing in the extract, and coverage on the steel surface increase [30, 31]. The results of Table 1 also indicate that for all concentrations performance of *Strychnos nux-vomica* extract in 4 % HCl is better than 8 % HCl. The maximum inhibition efficiency was obtained for concentration of 2 g L^{-1} of extract in both 4 % and 8 % HCl solution, and increasing the concentration does not create a significant change in the inhibition efficiency. Therefore, for electrochemical experiments which is discussed in the following, 2 g L^{-1} of *Strychnos nux-vomica* extract is the highest concentration that is examined.

3.1.2. The effect of immersion time

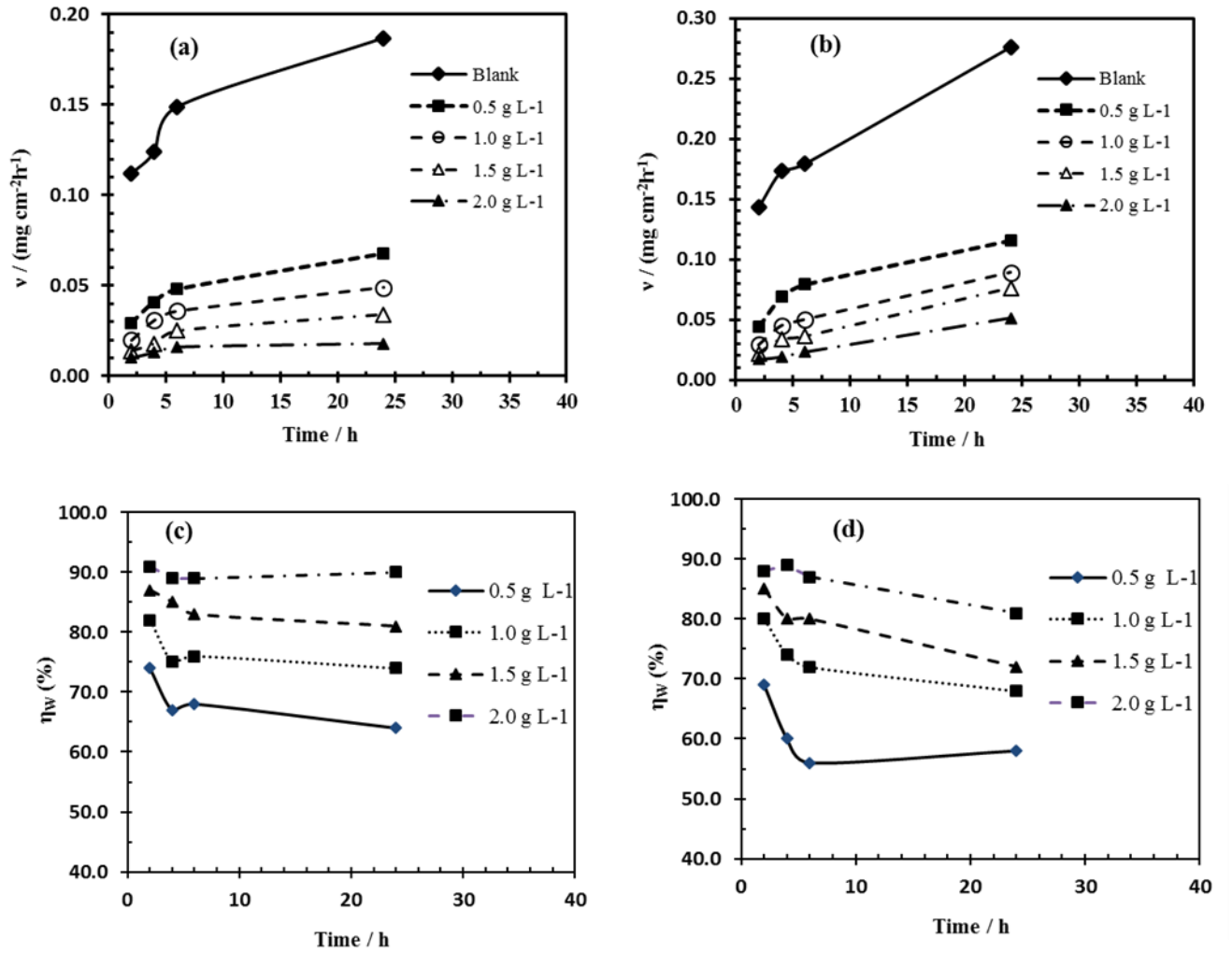

Figure 1. Variations of the corrosion rate (υ) and inhibition efficiency (η_w) with the immersion time without and with various concentrations of *Strychnos nux-vomica* extract in 4 % HCl (a and c) and 8 % HCl (b and d).

To investigate the stability and inhibition action of extracts in the time scale, weight loss tests in 4 % and 8 % HCl solution without and with different concentrations of *Strychnos nux-vomica* extract for immersion time ranges from 2 to 24 hours at 25 ° C were carried out. Fig. 1 (a and b) shows the weight loss-time curves and Fig. 1 (c and d) reviels the variation of η_w% with immersion time for carbon steel corrosion without and with varying concentrations of *Strychnos nux-vomica* extract. Fig.1 indicates that in both acid solution, the weight loss of carbon steel significantly enhanced with time in uninhibited solution compared to the inhibited solution. This is testifies to this reality that *Strychnos nux-vomica* extract actually inhibited the corrosion of carbon steel in both 4 % and 8 % HCl solution. It is clear from Fig. 1 (c and d) that the inhibition performance of *Strychnos nux-vomica* extract up to 24 hours of immersion in all of concentrations did not changed significantly.

3.2. Open circuit potential (E_{OCP})

To achieve steady state on the electrode surface, before each electrochemical test, the electrodes immersed in corrosive test solution and the open circuit potential (Eocp, vs.Ag/AgCl reference electrode) values observed with time. The results for various *Strychnos nux-vomica* extract concentrations and blank test solution.can be seen in Fig. 2. It could be observed from the figure that for both 4 % and 8 % HCl solution a stable OCP values were attained after 1000 s immersion in the absence and presence of the *Strychnos nux-vomica* extract. It is obvious from Fig. 2 that, the addition of *Strychnos nux-vomica* extract to the both HCl solution the E_{OCP} value shifted towards more positive values at all concentrations of *Strychnos nux-vomica* extrac, however, there was not a special relationship between E_{corr} and concentration. The classification of a compound as an anodic or cathodic type inhibitor is possible when the OCP displacement is at least 85 mV in relation to that one measured for the blank solution [32, 33]. The largest movement displayed by *Strychnos nux-vomica* extract in HCl solution relative to blank solution for 4 % HCl and 8 % HCl are 25 mV and 46 mV, respectively. Thus, it may be concluded that *Strychnos nux-vomica* extract in both 4 % HCl and 8 % HCl solutions performed as a mixed-type inhibitor.

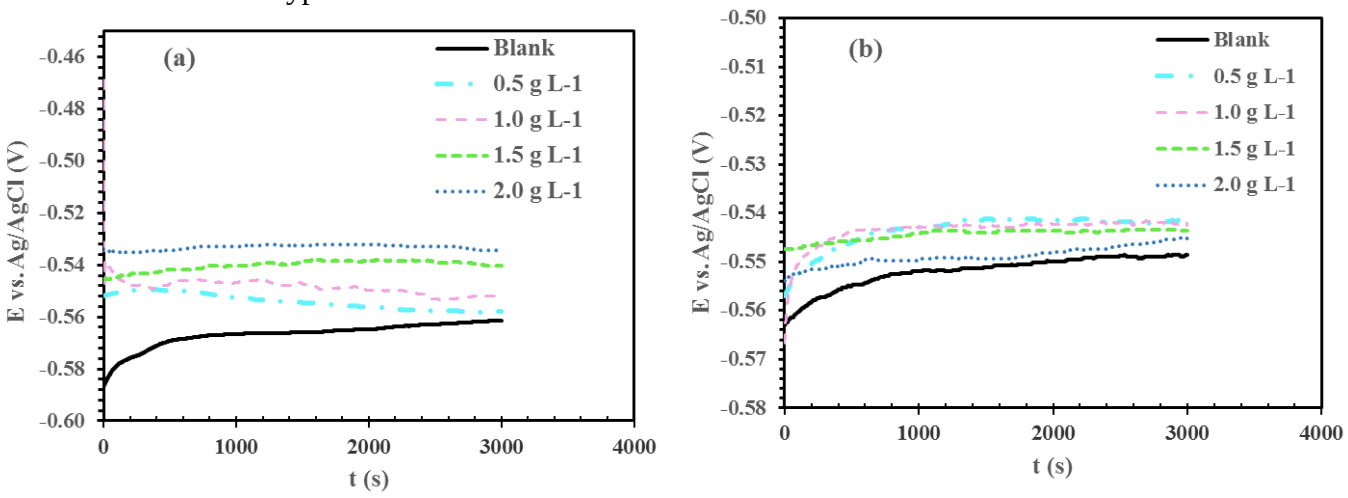

Figure 2. OCP plots for carbon steel in (a) 4 % HCl and (b) 8 % HCl without and with various concentration of *Strychnos nux-vomica* extract.

3.3. Potentiodynamic polarization measurements

The results of potentiodynamic polarization measurements for carbon steel in 4 % and 8 % HCl without and with various concentrations of *Strychnos nux-vomica* extract are displayed in Fig. 3. It is observed from Fig. 3 a and b that both cathodic and anodic branchs show a less current density in the presence of *Strychnos nux-vomica* extract than current density that recorded in the 4 % and 8 % HCl solution alone. This behavior indicated *Strychnos nux-vomica* extract has effect on both cathodic and anodic reactions.

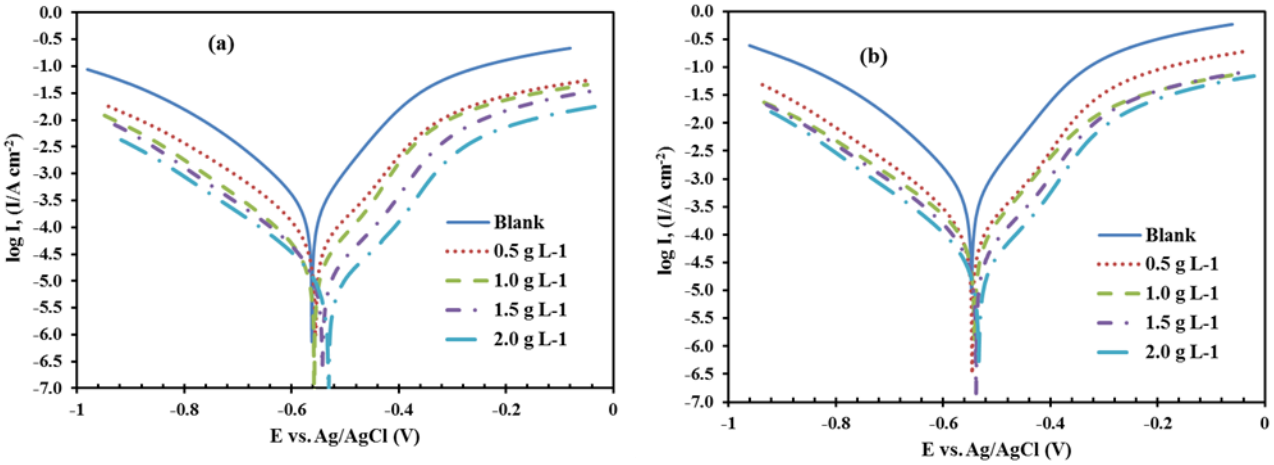

Figure 3. Potentiodynamic polarization graphs for the carbon steel in (a) 4 % HCl and (b) 8 % HCl with various concentration of *Strychnos nux-vomica* extract.

The electrochemical kinetic parameters such as corrosion current density (I_{corr}), corrosion potential (E_{corr}) and cathodic and anodic Tafel slopes (b_c *and* b_a) were defined from polarization curves and results are listed in Table 2.

Table 2. Polarization parameters for carbon steel in 4 % HCl and 8 % HCl in the presence and absence of *Strychnos nux-vomica* extract

Acid solution	Concentration (g L^{-1})	$-E_{corr}$ (V, vs. Ag/AgCl)	$-b_c$ (V dec^{-1})	b_a (V dec^{-1})	I_{corr} (μA cm^{-2})	η_{pol} (%)
4 % HCl	Blank	0.562	0.102	0.083	207.2	-
	0.5	0.555	0.114	0.115	64.3	68.97
	1.0	0.558	0.110	0.119	41.5	79.97
	1.5	0.541	0.117	0.091	32.5	84.31
	2.0	0.532	0.104	0.117	19.8	90.44
8 % HCl	Blank	0.547	0.096	0.089	488.3	-
	0.5	0.546	0.113	0.118	129.6	73.46
	1.0	0.561	0.126	0.113	83.7	82.86
	1.5	0.538	0.111	0.119	69.7	85.72
	2.0	0.534	0.106	0.122	48.5	90.06

Then, the obtained corrosion current density at different concentrations of *Strychnos nux-vomica* extract was used for calculating the inhibition efficiencies as the following equation [34, 35]:

$$\eta_{pol}(\%) = (\frac{I_0 - I}{I_0}) \times 100 \quad (4)$$

where I_0 and I are the corrosion current densities in uninhibited and inhibited solution, respectively.

According to Table 2, it becomes apparent that by increasing concentration of *Strychnos nux-vomica* extract corrosion current densities reduced and therefore inhibition efficiencies increase. This behavior returns the ability of *Strychnos nux-vomica* extract in order to inhibit the corrosion of carbon steel in both HCl media. It is obvious from potentiodynamic polarization graphs that the E_{corr} values in the presence of *Strychnos nux-vomica* extract shifted slightly toward positive direction, without any special relationship between E_{corr} and concentration, compared to uninhibited HCl solutions. The same results were obtained in OCP plot (in section 3.2.). The reason for these findings is attributed to the adsorption of compounds contained in extract at the active sites of steel surface. Thus, this effect causes the corrosion reaction is delayed [36]. Considering data in Table 2, after adding the extract, changes in the anodic and cathodic Tafel slopes is not significant. This suggests that molecules of *Strychnos nux-vomica* extract are adsorbed on the surface of carbon steel by simply blocking the active sites on the surface without altering the corrosion mechanism [37].

3.4. Electrochemical impedance spectroscopy measurements

Electrochemical impedance spectroscopy technique, represents a useful method for analyzing the characteristics of the surface of an electrode. Therefore, the phenomenon of inhibiting corrosion of carbon steel using *Strychnos nux-vomica* extract was investigated and quantified by this technique. Fig. 4 a and b illustrate the Nyquist plots of carbon steel in 4 % and 8 % HCl solution without and with *Strychnos nux-vomica* extract. The Nyquist plot of carbon steel in 4 % and 8 % HCl solution is given in the inset figure. The impedance spectra in both media exhibit one single depressed semicircle with the center under the real axis. The diameter of semicircle increases with the increase of *Strychnos nux-vomica* extract concentration that indicating strengthening of inhibitive film. The roughness and inhomogeneity of the surface of solid electrodes during corrosion cause depression in Nyquist plot of impedance spectra [20, 38]. The results obtained by electrochemical impedance spectroscopy are fitted to the electrical equivalent circuit showed in Fig. 4c. Where the equivalent circuit employed consists of R_s represents the solution resistance, R_{ct} indicative the charge transfer resistance and CPE indicative constant phase element to replace double layer capacitance (C_{dl}). The impedance (Z) of CPE is given with the expression [39, 40]

$$Z_{CPE} = Q^{-1}(j\omega)^{-n} \quad (5)$$

where Q is the CPE constant, ω is the angular frequency, $j^2 = -1$ is the imaginary number and n is the CPE exponent that can be offer more details about the degree of surface inhomogeneity resulting from surface roughness, porous layer formation, inhibitor adsorption etc [40]. The quantities obtained from fitting process are summarized in Table 3. Analyses of the impedance results in Table 3

illustrations that R_{ct} value increases with the concentration of *Strychnos nux-vomica* extract. The increase in R_{ct} values illustrate the enhanced protection properties of *Strychnos nux-vomica* extract and a slow corroding system, due to the gradual replacement of water molecules with inhibitor molecules on the surface and thus a decrease in the number of active sites for the corrosion reaction [13, 41]. The value of the CPE constant, *Q*, decreaced with inhibitor concentration.

The decreased Q can be related to the decreased dielectric constant and/or increased thickness of the double layer [42-44]. In the other words, in the presence of inhibitors, thickness of the surface oxide layer decreased and by changing in oxide layer the electrode process influence on the kinetics, thus, the value of *Q* reduced [2, 43, 45]. The lower value of n for 4 % and 8 % HCl solution compared with those in the inhibited solution demonstrate surface inhomogeneity due to roughening of steel surface as a result of corrosion. By adding the extract to the acidic media, the values of *n* increased which reflect the reduction of inhomogeneity of the surface because of adsorption of extract molecules on the steel surface [31].

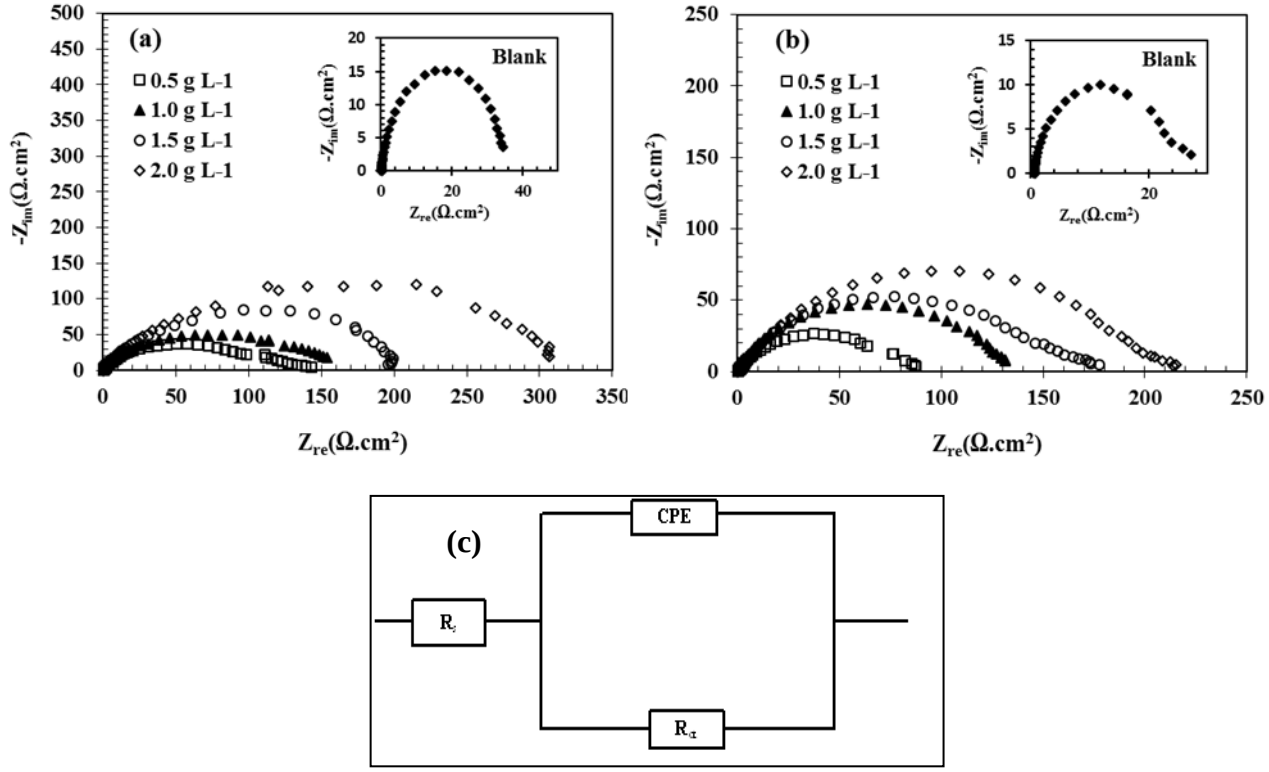

Figure 4. Nyquist plots for carbon steel (a) 4 % HCl, (b) 8 % HCl with different concentration of *Strychnos nux-vomica* extract and (c) The equivalent circuit model applied to recognize and fit EIS data.

The inhibition efficiencies for various concentrations of extract were calculated by using the following equation [46]:

$$\eta_{EIS}\,\% = \frac{R_{ct(inh)} - R_{ct}}{R_{ct(inh)}} \times 100 \qquad (6)$$

In equation (6), R_{ct} and $R_{ct\ (inh)}$ are the charge transfer resistance in the absence and presence of inhibitor, respectively [47]. The η_{EIS} (%) values derived from the EIS method are in good agreement with inhibition efficiency that obtained from the weight loss and the potentiodynamic polarization methods (Tables 1–3).

Table 3. Impedance data of carbon steel in 4 % HCl and 8 % HCl with and without *Strychnos nux-vomica* extract.

Acid solution	Concentration (g L^{-1})	R_s ($\Omega.cm^2$)	R_{ct} ($\Omega.cm^2$)	*CPE*		η_{EIS} (%)
				Q ($\mu\Omega^{-1}$ s^n cm^{-2})	n	
4 % HCl	Blank	0.65	35.1	5000.0	0.713	-
	0.5	0.22	117.4	161.0	0.723	70.1
	1.0	0.17	155.1	182.4	0.748	77.4
	1.5	0.22	208.3	92.9	0.870	83.1
	2.0	0.27	318.0	66.1	0.890	89.0
8 % HCl	Blank	0.54	23.5	105000.0	0.730	-
	0.5	0.14	82.0	42600.0	0.756	71.4
	1.0	0.17	130.8	99.5	0.802	82.1
	1.5	1.77	160.5	45.0	0.877	85.4
	2.0	2.60	205.0	43.7	0.878	88.6

3.4. Effect of temperature and activation parameters

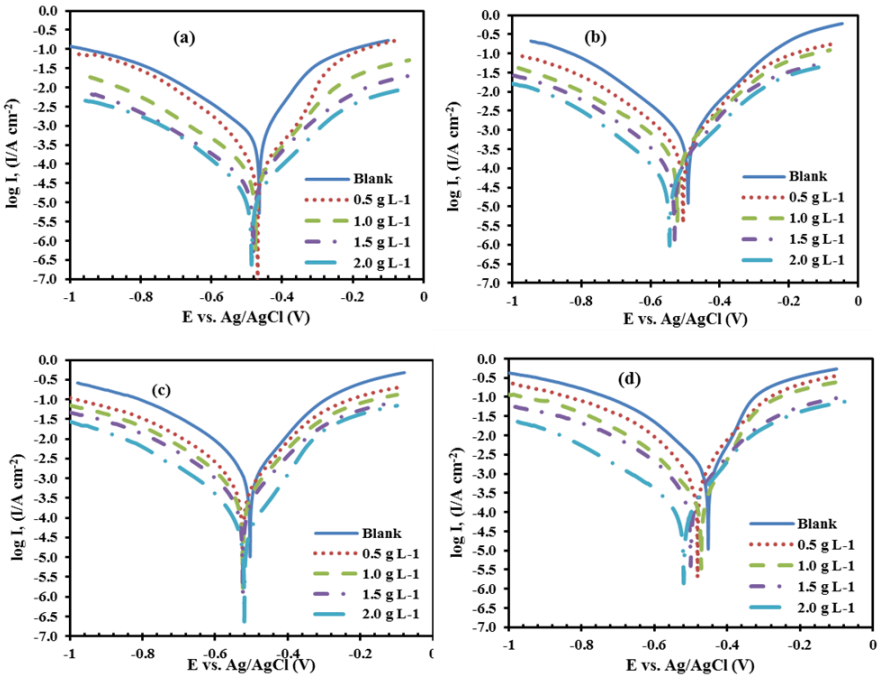

Figure 5. The effect of temperature on polarization curves of carbon steel corrosion rate in free (4 % HCl) and inhibited acid solutions; (a)35 °C, (b) 45 °C, (c) 55 °C and (d) 65 °C.

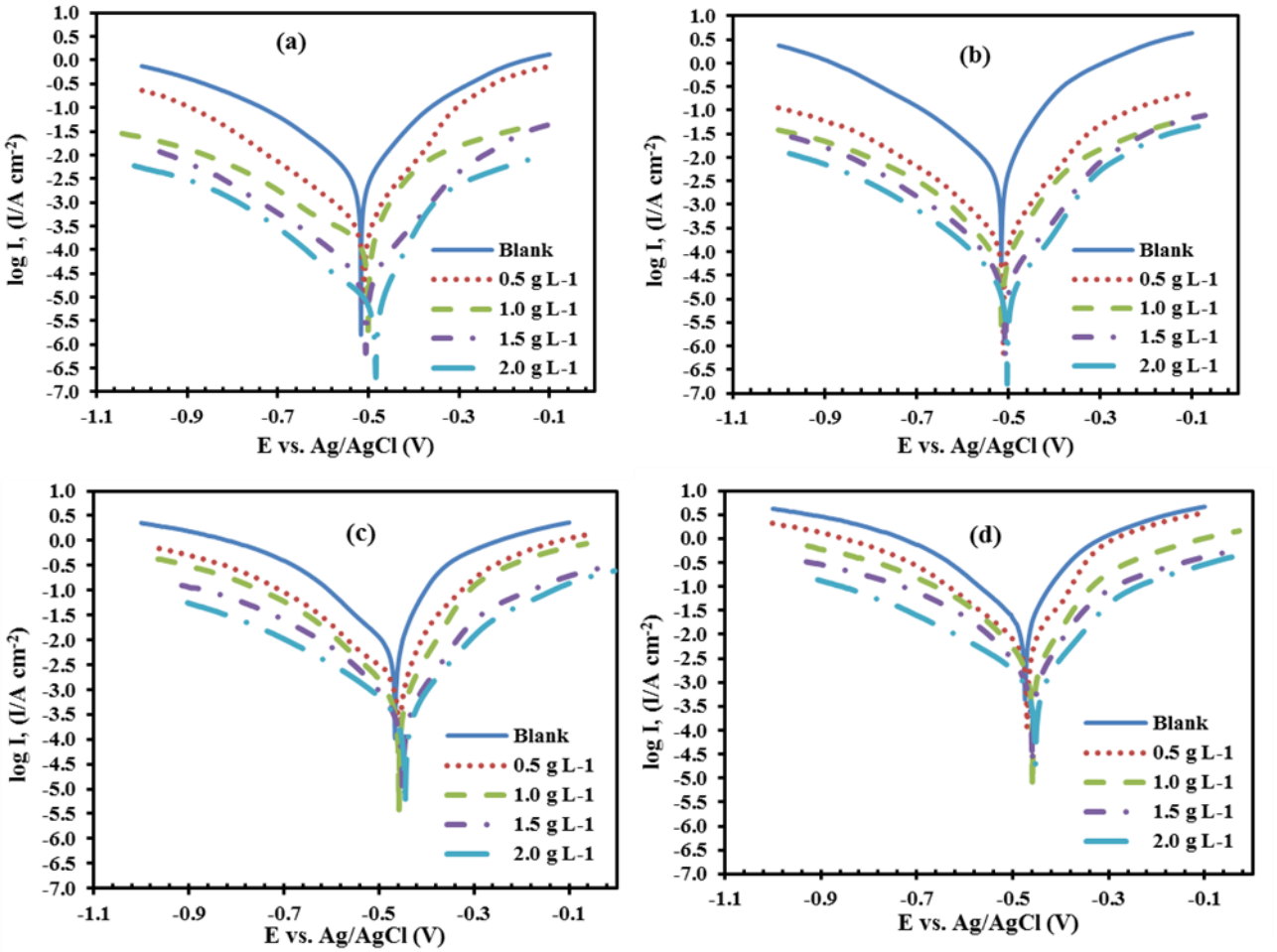

Figure 6. Effect of temperature on polarization curves of carbon steel corrosion rate in free (8 % HCl) and inhibited acid solutions; (a)35 °C, (b) 45 °C, (c) 55 °C and (d) 65 °C.

The potentiodynamic polarization measurements were performed at temperature range 35-65 °C, in order that assess the activation parameters for process of steel corrosion in both acidic solutions and also estimate the stability of adsorbed layer / film of the inhibitor on the surface of carbon steel. The polarization curves were achieved with and without various concentrations of the extract after 2 hours immersion at the desired temperature. The results are provided in Figs. 5 and 6 and Table 4. By examining the results of Table 4, it can be found that with increasing temperature, corrosion current density (I_{corr})enhanced and consequently, inhibition efficiency reduced. Although *Strychnos nux-vomica* extract has shown good inhibition properties at all studied temperatures. Reducing the inhibition efficiency by increasing the temperature have been attributed to acceleration of dissolution process of carbon steel and desorption of some molecules that adsorbed on the surface [26, 48].

Arrhenius (equation (7)) and transition state (equation (8)) were used for determination of activation parameters of corrosion process [21, 31]:

$$r = \lambda \exp(\frac{-E_a}{RT}) \quad (7)$$

$$r = \frac{RT}{N_A h}\exp(\frac{\Delta S^*}{R})\exp(-\frac{\Delta H^*}{RT}) \quad (8)$$

where λ *i*s the Arrhenius pre-exponential factor, T the absolute temperature, E_a the activation corrosion energy for the corrosion process, h the Planck's constant, N_A the Avogado's number, ΔS^* the entropy of activation, ΔH^* the enthalpy of activation and r is the rate of metal dissolution reaction that directly associated with corrosion current density (I_{corr}) [24, 31].

Table 4. Polarization parameters and equivalent inhibition efficiency of the carbon steel corrosion in 4 % HCl and 8 % HCl with and without *Strychnos nux-vomica* extract in various temperatures.

Temperature (ºC)	C (g L^{-1})	4 % HCl			8 % HCl		
		E_{corr} vs.Ag/AgCl (V)	I_{corr} (µA cm^{-2})	η_{pol} (%)	E_{corr} vs.Ag/AgCl (V)	I_{corr} (µA cm^{-2})	η_{pol} (%)
35	Blank	-0.485	422.1	-	-0.516	729.2	-
	0.5	-0.47	179.6	57.5	-0.509	236.6	67.6
	1.0	-0.476	115.6	72.6	-0.500	163.6	77.6
	1.5	-0.482	75.7	82.1	-0.506	152.2	79.1
	2.0	-0.486	59.9	85.8	-0.484	85.7	88.2
45	Blank	-0.491	728.8	-	-0.515	996.2	
	0.5	-0.507	342.3	53.0	-0.510	383.1	61.5
	1.0	-0.522	257.8	64.6	-0.514	285.3	71.4
	1.5	-0.531	129.3	82.3	-0.507	236.4	76.3
	2.0	-0.545	113.6	84.4	-0.502	143.6	85.6
55	Blank	-0.504	1358.0	-	-0.466	2344.1	-
	0.5	-0.529	694.2	48.9	-0.456	994.2	57.6
	1.0	-0.525	472.2	65.2	-0.457	741.4	68.4
	1.5	-0.525	294.7	78.3	-0.450	587.6	74.9
	2.0	-0.521	231.8	82.9	-0.444	453.7	80.6
65	Blank	-0.452	1715.3	-	-0.474	3897.2	-
	0.5	-0.482	926.3	46.0	-0.469	1811.8	53.5
	1.0	-0.472	657.8	61.7	-0.459	1424.7	63.4
	1.5	-0.500	377.8	78.0	-0.458	1105.2	71.6
	2.0	-0.519	316.2	81.6	-0.554	874.2	77.6

By drawing ln I_{corr} against $10^3/T$, a straight line with a slope of ($-E_a$/R) obtained. Thereby, the apparent activation energy of corrosion reaction in uninhibited and inhibited acid solution can be calculated. Fig. 7 (a and c) displays the Arrhenius plots in the absence and presence of different concentrations of *Strychnos nux-vomica* extract. The corresponding values of E_a are given in Table 5 and indicate that values of E_a obtained in solutions containing *Strychnos nux-vomica* extract are higher than those in uninhibited acid solutions. Increasing E_a for dissolution of carbon steel in solution containing *Strychnos nux-vomica* has been interpreted as physical adsorption in the first step [25, 26, 49]. Szauer and Brand [30] explained that the increase in activation energy can be attributed to an appreciable decrease in the adsorption of the inhibitor on the carbon steel surface with the increase in temperature.

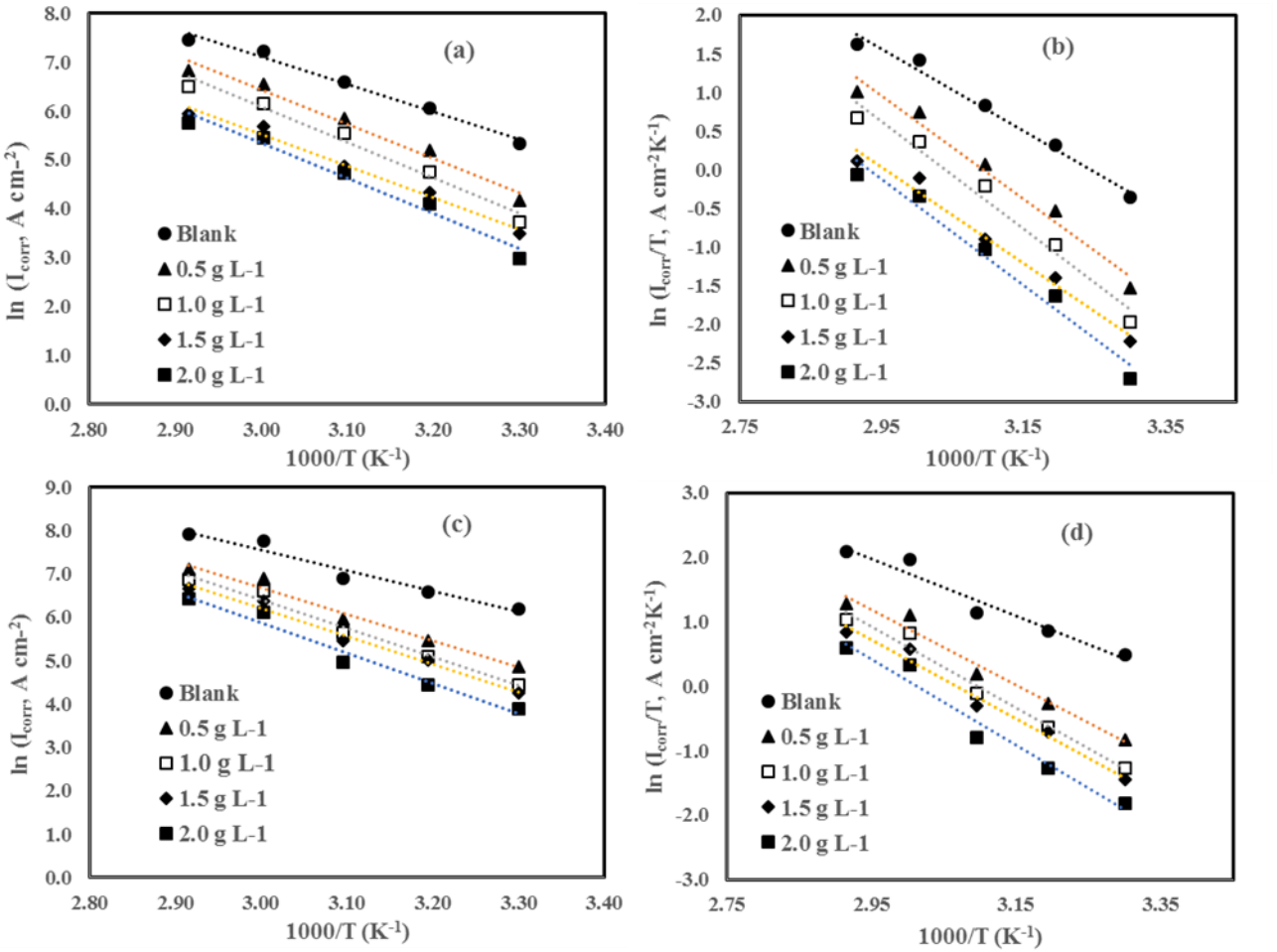

Figure 7. Arrhenius plots of (a and c) ln I_{corr} versus 1/T and (b and d) ln (I_{corr}/T) versus 1/T in the absence and presence of different concentration of *Strychnos nux-vomica* extract in (a and b) 4 % HCl, (c and d) 8% HCl.

The ΔH^* and ΔS^* values were calculated by using plot of ln (I_{corr}/T) against $10^3/T$ that shown in Fig. 7 (b and d). The result is a straight line with a slope of ($-\Delta H^*/R$) and intercept equal to $[\ln(\frac{R}{Nh}) + (\frac{\Delta S^*}{R})]$. The ΔH^* and ΔS^* values are displayed in Table 5. The result of Table 5 show that signs of ΔH^* are positive, this means the process of steel dissolution is endothermic and dissolution of steel is difficult [50]. It is also noteworthy that the values of E_a and ΔH^* vary in the same way. This result clear the known thermodynamic reaction between the E_a and ΔH^* ($E_a - \Delta H^* = RT$) and the values are very close to RT which is 2.48 kJ/mol at 298 K as shown in Table 5. Large and negative values of entropies ΔS^* suggest that in the rate determining step the activated complex displaies an association rather than a dissociation step, this means that disordering reduced when going from reactants to the activated complex [31, 32, 51].

Table 5. Activation parameters, E_a, ΔH^*, ΔS^*, of the dissolution of carbon steel in 4 % and 8 %HCl without and with *Strychnos nux-vomica* extract.

Acid solution	Concentration (g L^{-1})	E_a (kJ mol^{-1})	ΔH^* (kJ mol^{-1})	ΔS^* (J $mol^{-1}K^{-1}$)
4 % HCl	Blank	46.8	44.1	-54.4
	0.5	58.1	55.4	-26.1
	1.0	60.3	57.6	-22.5
	1.5	54.3	51.6	-44.9
	2.0	59.9	57.2	-29.7
8 % HCl	Blank	39.7	37.0	-72.0
	0.5	51.3	48.6	-44.4
	1.0	55.2	52.5	-34.9
	1.5	53.5	50.7	-41.9
	2.0	58.2	55.5	-30.3

3.5. Adsorption isotherm

In general, the initial step in behavior of inhibitors in acidic solutions is attributed to adsorption onto the metal surface. This includes assuming that the active sites over the area of the metal surface were covered with inhibitor molecules through adsorption on the surface, therefore, the corrosion process can be prevented [33]. In order to appreciate the mechanism of adsorption, adsorption behavior of organic compounds described using adsorption isotherm. Several adsorption isotherms such as Langmuir, Freundlich,Temkin, Flory–Huggins and Bockris–Swinkels isotherms can be used to assess the adsorption behaviour of the inhibitors with the value of correlation coefficient (R^2) as a estimate to define the best fit adsorption isotherm. Langmuir adsorption isotherm characterized by equation (9) was found to be the best fit from all the tested isotherms.

$$\frac{C_{inh}}{\theta} = \frac{1}{K_{ads}} + C_{inh} \qquad (9)$$

where C_{inh}, θ and K_{ads} are the extract concentration, degree of surface coverage and equilibrium constant of adsorption–desorption process, respectively. The values of θ for different concentrations at different temperatures have been estimated from the potentiodynamic polarization data by using inhibition efficiency (η_{pol}) as $\theta = \eta_{pol}/100$. The relation between C/θ and C at different temperatures is displayed in Fig. 8. The parameters of adsorption constant, slope, and linear correlation coefficient (R^2) are available from the regressions between C/θ and C, and the results are shown in Table 6. The slope of these linear equations is equal to unity. This isotherm assumes that the adsorbed molecules existing in the *Strychnos nux-vomica* extract occupy only one site and there are no interactions with other adsorbed molecules [36, 52]. The adsorptive equilibrium constant (K_{ads}) is related to the standard adsorption free energy (ΔG^0_{ads}) obtained according to[38, 53]:

$$K_{ads} = (\frac{1}{55.5}) \exp(\frac{-\Delta G^0_{ads}}{RT}) \qquad (10)$$

where R is gas constant and T is absolute temperature of experiment and the constant value of 55.5 is the concentration of water in solution in mol dm^{-3}.

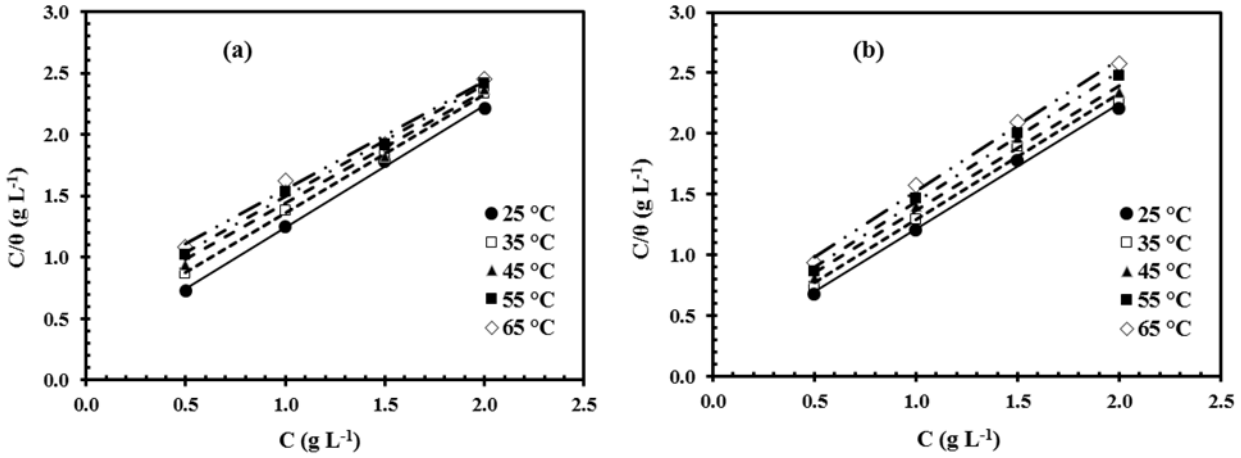

Figure 8. Langmuir isotherm for adsorption of *Strychnos nux-vomica* extract in (a) 4 % and (b) 8 % HCl solution on the carbon steel surface.

The calculated K_{ads} and ΔG^0_{ads} results are also listed in Table 6. It was described that values of ΔG^0_{ads} up to -20 kJ mol^{-1} are consistent with the electrostatic interaction between the charged molecules and the unlike charged metal (physical adsorption) while those more negative than about -40 kJ mol^{-1} involve sharing or transfer of electrons from the inhibitor molecules to the metal surface to form a coordinate bond (chemisorption) [13, 54, 55]. Inspection of Table 6 discloses that the ΔG^0_{ads} at all temperatures is lower than -20 kJ mol^{-1}. Therefore, it is decided that physical adsorption interactions must be predominant for the adsorption molecules existing in the *Strychnos nux-vomica* extract on the surface of carbon steel.

Table 6. Thermodynamic parameters for the adsorption of *Strychnos nux-vomica* extract in 4 % and 8 % HCl on the carbon steel at different temperatures.

Acid solution	4% HCl					8% HCl				
Temperature (ºC)	25	35	45	55	65	25	35	45	55	65
Slope	0.9975	0.9664	0.9111	0.9098	0.8793	1.0328	1.0370	1.0277	1.0749	1.0899
R^2	0.9978	0.9995	0.9823	0.9972	0.9892	0.9970	0.9910	0.9899	0.9977	0.9956
K_{ads}	4.09	2.54	1.88	1.71	1.49	5.60	3.97	2.90	2.78	2.31
ΔG^0_{ads} (kJ mol^{-1})	-13.44	-12.67	-12.29	-12.42	-12.40	-14.22	-13.82	-13.43	-13.74	-13.64
ΔH^0_{ads} (kJ mol^{-1})	-20.44	-20.44	-20.44	-20.44	-20.44	-17.96	-17.96	-17.96	-17.96	-17.96
ΔS^0_{ads} (J mol^{-1} K^{-1})	-23.50	-25.24	-25.64	-24.46	-23.80	-12.54	-13.43	-14.24	-12.86	-12.77

Van't Hoff equation (Eq. 11) and then rearranged equation derived from it (Eq. 12) can be used to calculate the standard adsorption enthalpy (ΔH^0_{ads}) as the following [42, 43]:

$$\frac{d \ln K_{ads}}{dT} = \frac{\Delta H^0_{ads}}{RT^2} \quad (11)$$

$$\ln K_{ads} = \frac{-\Delta H^0_{ads}}{RT} + D \quad (12)$$

where R, T and K_{ads} are the same concepts that are presented (in equations 9 and 10) in Section 3-5 and D is integration constant. Fig. 9 illustrates the straight line of ln K_{ads} versus 1/T with a slope of ($-\Delta H^0_{ads}$/R). Thereby the values of ΔH^0_{ads} were determined and the results are presented in Table 6. Tests performed at the atmospheric pressure and a very low concentration solution that is close to standard conditions, therefore, the standard adsorption heat ΔH^0_{ads} can be usable instead the adsorption heat ΔH_{ads} [2, 56]. By using the values of ΔH_{ads} can be judged about type of adsorption (chemisorption, physisorption or a mixture of both) as following [47, 57]:

- The endothermic adsorption process ($\Delta H_{ads} > 0$) is attributed unequivocally to chemisorption
- The exothermic adsorption process ($\Delta H_{ads} < 0$) may include chemisorption, physisorption or a mixture of both. So that by considering the absolute value of ΔH_{ads} the value less than 40 kJ/mol is physisorption, while the value approaches 100 kJ/mol is chemisorptions [48, 57].

According to the aforementioned points and the rsults of Table 6, the sign of ΔH_{ads} is negative designated that the adsorption of *Strychnos nux-vomica* extract in both HCl solutions is exothermic.

The absolute values of ΔH_{ads} for adsorption of *Strychnos nux-vomica* extract in 4 % and 8 % HCl are 20.44 and 17.96 kJ/mol, respectively, which are lower than 40 kJ/mol and suggests that physisorption occurs.

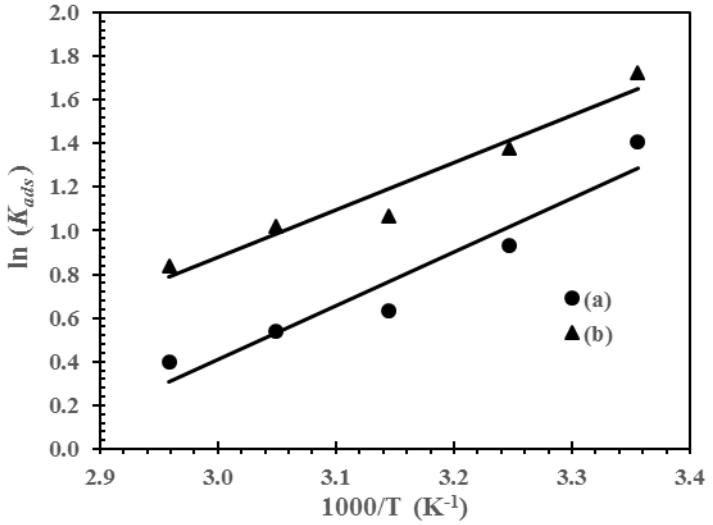

Figure 9. The relationship between ln K_{ads} and 1/T for carbon steel for *Strychnos nux-vomica* extract in (a) 4 % and (b) 8 % HCl solution.

With the obtained both parameters of ΔG^0_{ads} and ΔH^0_{ads}, entropy of adsorption (ΔS^0_{ads}) can be calculated using the following equation:

$$\Delta G^0_{ads} = \Delta H^0_{ads} - T\Delta S^0_{ads} \quad (13)$$

The calculated ΔS^0_{ads} data are shown in Table 6. All obtained data are negative demonstrating that, the entropy of molecules of *Strychnos nux-vomica* extract in the solution phase is higher than solid phase [37].

3.6. Quantum chemical studies and adsorption mechanism

The experimental results obviously presented that the inhibition mechanism of *S. nux-vomica* extract related to adsorption of molecules, available at it, on the metal surface. In the adsorption phenomenon, the molecules and metal behave as a Lewis base and Lewis acid, respectively. On the other hand, the interaction between molecules and metal was accomplished with overlap of frontier orbitals through the sharing of electrons of molecules and the partially filled d-orbitals of the metal. As a result we have this thought that maybe quantum chemical calculation can guidance to predict adsorption inhibitor molecules on the surface of metal. Because of the large number of compounds in the extract, assign the inhibition effect it to a specific compound seems to be difficult. But the quantum chemical calculations is applicable only for a compound. So, we chose the main components of the extract for quantum chemical studies. The major components from *S. nux-vomica* seed extract were reported to be strychnine and brucine type alkaloids whose structures are given in Fig. 10 [58]. Therefore, these two compounds were selected for quantum chemical studies.

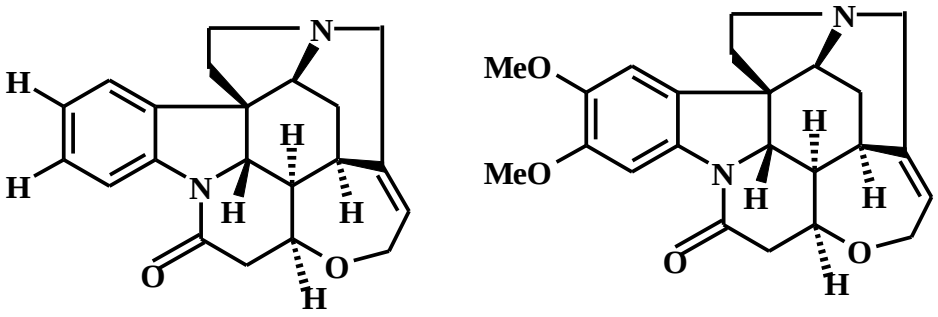

Strychnine **Brucine**

Figure 10. The structures of strychnine and brucine.

The optimized molecular structures, the frontier molecule orbital density distribution (highest occupied molecular orbital (HOMO) and the lowest unoccupied molecular orbital (LUMO)) of strychnine and brucine are presented in Fig. 11. The quantum chemical indices such as the energy of the highest occupied molecular orbital (E_{HOMO}), the energy of the lowest unoccupied molecular orbital

(E_{LUMO}) and energy band gap, $\Delta E = E_{HOMO} - E_{LUMO}$ were obtained for strychnine and brucine. The values of E_{HOMO}, E_{LUMO} and ΔE are -0.32159, 0.00788 and 0.32947 for strychnine and these value for brucine are -0.30179, 0.00838 and 0.31017, respectively. The higher value of E_{HOMO} indicate that molecule is much more willing to donate electrons to a suitable acceptor by vacant molecular orbital. The lower value of ΔE for a molecule will lead to better performance as inhibitor, because the energy required to remove an electron from last occupied orbitals are minimized. The amount of E_{HOMO} for brucine is higher than strychnine and the amount of ΔE for brucine is lower than strychnine. So it seems that the inhibition action of brucine is better than strychnine.

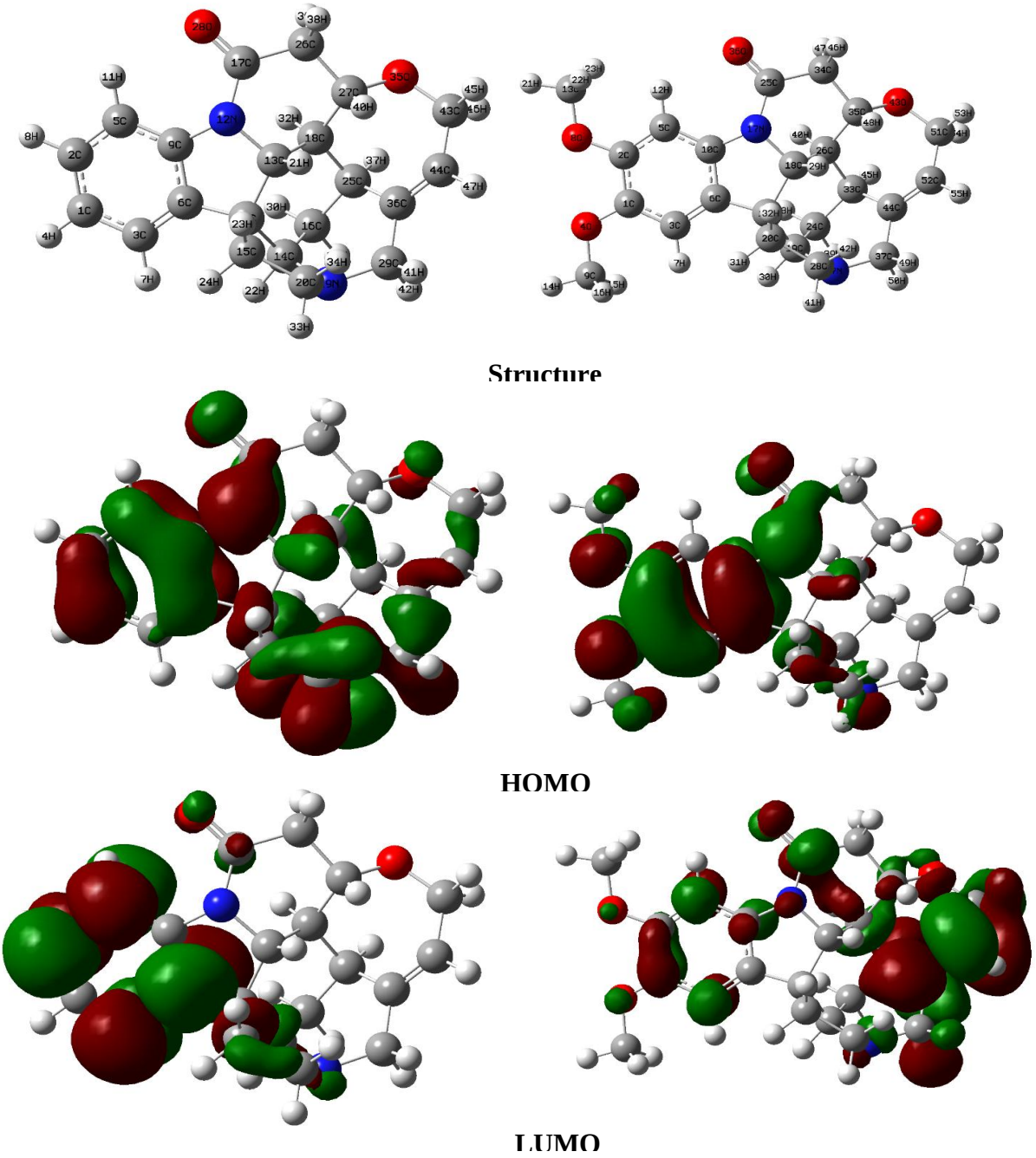

Figure 11. The optimization geometry, HOMO and LUMO density of strychnine (left side) and brucine (right side).

The frontier molecule orbital density distribution HOMO and LUMO were applied for assumption of the adsorption sites and state of adsoption of strychnine and brucine on the surface of steel. The only difference in structure of molecules strychnine and brucine arises from the substitutions OCH_3 on the benzene ring of brucine. As can be seen in the figure 11, the HOMO and LUMO orbitals for strychnine and brucine are localized around nitrogen atoms, oxygen atoms, carbon-carbon double bonds and aromatic ring. Therefore, strychnine and brucine through these locations may be interact with the steel surface. This is shown schematically in Fig. 12. It seems that, the presence of additional groups of OCH_3 in the brucine lead to stronger interaction of it with the metal surface. As a result, surface coating through brucine is better than strychnine. In the end, we noted that a large number of the molecules present in extract that can be adsoption on the surface of metal and protect the metal from the aggressive environment. Even the synergistic effect of these compounds may also improve the performance of any of the molecules compared to when they are used alone.

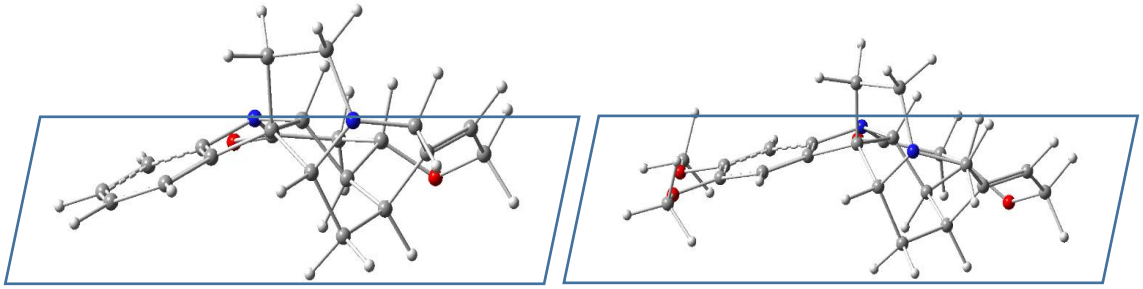

Figure 12. Schematically adsorption behavior of strychnine (left side) and brucine (right side) On the carbon steel surface.

4. CONCLUSIONS

The main conclusions are as follows:

1. *S. nux-vomica* extract is suitable for inhibition of corrosion carbon steel in 4 % and 8 % HCl. The amount of η % achieved from weight loss, potentiodynmic polarization and EIS are in good agreement with each other. Meanwhile, in all three methods, η % increased by increasing concentration of S. nux-vomica extract.
2. Polarization curves measurements indicate that *S. nux-vomica* extract treated as mixed type inhibitor in both 4 % and 8 % HCl solutions.
3. The reason for inhibition action of *S. nux-vomica* extract can be attributed to the adsorption of molecules existing in the extract on the carbon steel surface and protect it from corrosion.
4. The adsorption of S. nux-vomica extract at all studied temperatures was described by Langmuir isotherm model.
5. Thermodynamic adsorption parameters indicate that the adsoption of molecules of S. nux-vomica extract are a spontaneous exothermic process and a physisorption process can be proposed for that.

ACKNOWLEDGEMENT
The financial support of research council of Payame Noor University of Isfahan is gratefully acknowledged.

References

1. M. Migahed, I. Nassar, *Electrochim. Acta*, 53 (2008) 2877-2882.
2. T. Zhao, G. Mu, *Corros. Sci.*, 41 (1999) 1937-1944.
3. A.K. Singh, M. Quraishi, *Corros. Sci.*, 53 (2011) 1288-1297.
4. B.D. Mert, M. Erman Mert, G. Kardaş, B. Yazıcı, *Corros. Sci*., 53 (2011) 4265-4272.
5. E.A. Flores, O. Olivares, N.V. Likhanova, M.A. Domínguez-Aguilar, N. Nava, D. Guzman-Lucero, M. Corrales, *Corros. Sci.*, 53 (2011) 3899-3913.
6. A. Pourghasemi Hanza, R. Naderi, E. Kowsari, M. Sayebani, *Corros. Sci.*, 107 (2016) 96-106.
7. J. Cruz, R. Martınez, J. Genesca, E. Garcıa-Ochoa, *J. Electroanal. Chem.*, 566 (2004) 111-121.
8. A. Yurt, A. Balaban, S.U. Kandemir, G. Bereket, B. Erk, *Mater. Chem. Phys.*, 85 (2004) 420-426.
9. J.M. Roque, T. Pandiyan, J. Cruz, E. García-Ochoa, *Corros. Sci.*, 50 (2008) 614-624.
10. M. Belayachi, H. Serrar, H. Zarrok, A. El Assyry, A. Zarrouk, H. Oudda, S. Boukhris, B. Hammouti, E.E. Ebenso, A. Geunbour, *Int. J. Electrochem. Sci.*, 10 (2015) 3010-3025.
11. P. Morales-Gil, M.S. Walczak, C.R. Camargo, R.A. Cottis, J.M. Romero, R. Lindsay, *Corros. Sci.*, 101 (2015) 47-55.
12. P. Morales-Gil, M.S. Walczak, R.A. Cottis, J.M. Romero, R. Lindsay, *Corros. Sci*., 85 (2014) 109-114.
13. S. Deng, X. Li, *Corros. Sci*., 64 (2012) 253-262.
14. O.K. Abiola, A. James, *Corros. Sci.*, 52 (2010) 661-664.
15. K. Anuradha, R. Vimala, B. Narayanasamy, J. Arockia Selvi, S. Rajendran, *Chemical Engineering Communications*, 195 (2007) 352-366.
16. A. Badiea, K. Mohana, *Journal of Materials Engineering and Performance*, 18 (2009) 1264-1271.
17. A. El-Etre, *J. Colloid Interface Sci*., 314 (2007) 578-583.
18. E. Oguzie, C. Enenebeaku, C. Akalezi, S. Okoro, A. Ayuk, E. Ejike, *J. Colloid Interface Sci*., 349 (2010) 283-292.
19. L. Li, X. Zhang, J. Lei, J. He, S. Zhang, F. Pan, *Corros. Sci.*, 63 (2012) 82-90.
20. J.C. da Rocha, J.A.d.C.P. Gomes, E. D'Elia, *Corros. Sci*., 52 (2010) 2341-2348.
21. M. Behpour, S. Ghoreishi, M.K. Kashani, N. Soltani, *Materials and corrosion*, 60 (2009) 895-898.
22. H. Gerengi, H.I. Sahin, *Industrial & Engineering Chemistry Research*, 51 (2011) 780-787.
23. M. Behpour, S.M. Ghoreishi, M. Khayatkashani, M. Motaghedifard, *Phytochemical Analysis*, 23 (2012) 95-102.
24. G. Achary, H. Sachin, Y.A. Naik, T. Venkatesha, *Mater. Chem. Phys.*, 107 (2008) 44-50.
25. L. Larabi, O. Benali, Y. Harek, *Mater. Lett.*, 61 (2007) 3287-3291.
26. A. Singh, I. Ahamad, V. Singh, M.A. Quraishi, *J. Solid State Electrochem.*, 15 (2011) 1087-1097.
27. M.J. Frisch, G.W. Trucks, H.B. Schlegel, G.E. Scuseria, M.A. Robb, J.R. Cheeseman, J.A. Montgomery, Jr., T. Vreven, K.N. Kudin, J.C. Burant, J.M. Millam, S.S. Iyengar, J. Tomasi, V. Barone, B. Mennucci, M. Cossi, G. Scalmani, N. Rega, G.A. Petersson, H. Nakatsuji, M. Hada, M. Ehara, K. Toyota, R. Fukuda, J. Hasegawa, M. Ishida, T. Nakajima, Y. Honda, O. Kitao, H. Nakai, M. Klene, X. Li, J.E. Knox, H.P. Hratchian, J.B. Cross, C. Adamo, J. Jaramillo, R. Gomperts, R.E. Stratmann, O. Yazyev, A.J. Austin, R. Cammi, C. Pomelli, J.W. Ochterski, P.Y. Ayala, K. Morokuma, G.A. Voth, P. Salvador, J.J. Dannenberg, V.G. Zakrzewski, S. Dapprich, A.D. Daniels, M.C. Strain, O. Farkas, D.K. Malick, A.D. Rabuck, K. Raghavachari, J.B. Foresman, J.V. Ortiz, Q. Cui, A.G. Baboul, S. Clifford, J. Cioslowski, B.B. Stefanov, G. Liu, A. Liashenko, P. Piskorz, I. Komaromi, R.L. Martin, D.J. Fox, T. Keith, M.A. Al-Laham, C.Y. Peng, A. Nanayakkara, M.

Challacombe, P.M.W. Gill, B. Johnson, W. Chen, M.W. Wong, C. Gonzalez, J.A. Pople, Gaussian 03, Revision C.02, Gaussian, Inc., Wallingford, CT, 2004.
28. L. Tang, X. Li, L. Li, G. Mu, G. Liu, *Surface and Coatings Technology*, 201 (2006) 384-388.
29. L. Tang, X. Li, G. Mu, G. Liu, L. Li, H. Liu, Y. Si, *Journal of materials science*, 41 (2006) 3063-3069.
30. T. Szauer, A. Brandt, *Electrochim. Acta*, 26 (1981) 1253-1256.
31. N. Soltani, N. Tavakkoli, M. Khayatkashani, M.R. Jalali, A. Mosavizade, *Corros. Sci.*, 62 (2012) 122-135.
32. M. Behpour, S. Ghoreishi, M. Khayatkashani, N. Soltani, *Corros. Sci.*, 53 (2011) 2489-2501.
33. E.A. Noor, *Mater. Chem. Phys.*, 114 (2009) 533-541.
34. N. Soltani, N. Tavakkoli, M. Khayat Kashani, A. Mosavizadeh, E.E. Oguzie, M.R. Jalali, *Journal of Industrial and Engineering Chemistry*, 20 (2014) 3217-3227.
35. K.C. Emregül, M. Hayvalí, *Corros. Sci.*, 48 (2006) 797-812.
36. S.A. Ali, M. Saeed, S. Rahman, *Corros. Sci.*, 45 (2003) 253-266.
37. H. Ashassi-Sorkhabi, B. Shaabani, D. Seifzadeh, *Appl. Surf. Sci.*, 239 (2005) 154-164.
38. X. Li, S. Deng, H. Fu, G. Mu, *Corros. Sci.*, 51 (2009) 620-634.
39. N.A. Negm, N.G. Kandile, E.A. Badr, M.A. Mohammed, *Corros. Sci.*, 65 (2012) 94-103.
40. P.M. Krishnegowda, V.T. Venkatesha, P.K.M. Krishnegowda, S.B. Shivayogiraju, *Industrial & Engineering Chemistry Research*, 52 (2013) 722-728.
41. R. Solmaz, G. Kardaş, M. Culha, B. Yazıcı, M. Erbil, *Electrochim. Acta*, 53 (2008) 5941-5952.
42. G. Mu, X. Li, G. Liu, *Corros. Sci.*, 47 (2005) 1932-1952.
43. W. Durnie, B. Kinsella, R. De Marco, A. Jefferson, *J. Appl. Electroch.*,, 31 (2001) 1221-1226.
44. B. Zhang, C. He, C. Wang, P. Sun, F. Li, Y. Lin, *Corros. Sci.*, 94 (2015) 6-20.
45. B. Zhang, C. He, X. Chen, Z. Tian, F. Li, *Corros. Sci.*, 90 (2015) 585-596.
46. S. John, A. Joseph, *Research on Chemical Intermediates*, 38 (2012) 1359-1373.
47. F. Bentiss, M. Lebrini, M. Lagrenée, *Corros. Sci.*, 47 (2005) 2915-2931.
48. E.A. Noor, A.H. Al-Moubaraki, *Mater. Chem. Phys.*, 110 (2008) 145-154.
49. M. Larif, A. Elmidaoui, A. Zarrouk, H. Zarrok, R. Salghi, B. Hammouti, H. Oudda, F. Bentiss, *Research on Chemical Intermediates*, 39 (2013) 2663-2677.
50. A.K. Singh, S.K. Shukla, M. Singh, M. Quraishi, *Mater. Chem. Phys.*, 129 (2011) 68-76.
51. G.K. Gomma, M.H. Wahdan, *Mater. Chem. Phys.*, 39 (1995) 209-213.
52. M. Behpour, S. Ghoreishi, M. Khayatkashani, N. Soltani, *Mater. Chem. Phys.*, 131 (2012) 621-633.
53. R. Fuchs-Godec, V. Doleček, *Colloids and Surfaces A: Physicochemical and Engineering Aspects*, 244 (2004) 73-76.
54. A. Fouda, F. Heakal, M. Radwan, *J. Appl. Electroch.*, 39 (2009) 391-402.
55. N. Soltani, M. Behpour, E. Oguzie, M. Mahluji, M. Ghasemzadeh, *RSC Advances*, 5 (2015) 11145-11162.
56. A. El-Tabei, M. Hegazy, *Journal of Surfactants and Detergents*, 16 (2013) 757-766.
57. J. Aljourani, K. Raeissi, M. Golozar, *Corros. Sci.*, 51 (2009) 1836-1843.
58. N. Bisset, J. Phillipson, The Asian species of strychnos. Part IV. The alkaloids, Lloydia, 39 (1975) 263-325.